Power Flow Tracing of Renewable Energy Sources Through Lens of Transportation Network Modeling

Saman Mazaheri Khamaneh
Civil, Environmental, and Construction Engineering
University of Central Florida
Orlando, Florida, USA
smazaheri@ucf.edu

Zhaomiao Guo
Civil, Environmental, and Construction Engineering
University of Central Florida
Orlando, Florida, USA
guo@ucf.edu

2024 IEEE Kansas Power and Energy Conference (KPEC) | 979-8-3503-7240-3/24/$31.00 ©2024 IEEE | DOI: 10.1109/KPEC61529.2024.10676134

***Abstract*—Policies have been developed to incentivize the integration of renewable energy sources (RESs) in the power sector, which requires proper tracing and tracking of energy sources. However, power flow tracing (PFT) is fundamentally challenging due to the homogeneous nature of electricity and the interconnection of power systems. This paper proposes a path-based optimization approach for PFT that can effectively calculate the upper and lower bounds of origin-destination (OD) flow in power distribution systems (DSs). We demonstrate our methodology in the context of "green hydrogen" to estimate the potential range of specific energy sources for hydrogen production. The approach is validated using the IEEE-33 node DS to draw practical insights. The proposed methodology can be used to verify the amount of "green hydrogen" production eligible for government credits and guide the facility siting of hydrogen production facilities to maximize the integration of renewable energy resources.**

***Index Terms*—Power flow tracing, renewable energy sources, origin-destination estimation, convex optimization, hydrogen production**

I. Introduction

The reduction of carbon emissions in the energy sector has become a central theme for the sustainable development of society. Hydrogen production via electrolysis, powered by renewable energy sources (RESs), has emerged as a promising technology for achieving a net-zero carbon emission [1]. Governments have implemented a range of incentives and tax credits to support this transition. For example, the Inflation Reduction Act of 2022 introduces significant tax incentives incentivizing industries to use clean energy in hydrogen production [2]. In this regard, a proper methodology to trace and track the power sources becomes prominent to justify the claimed tax credits.

However, due to the homogeneous nature of electricity and the interconnectivity of the power grid, power flow tracing (PFT) is challenging. The concept of PFT has its roots in the early days of electrical power systems, where the need to allocate costs and understand the flow of electricity emerged. Numerous methodologies have been proposed to facilitate PFT calculation. The proportional sharing principle (PSP), a conventional approach introduced by [3] and further developed in recent studies (e.g., [4]–[6]), assumes a proportional distribution among the outflows of buses. Although intuitive, the simplification of power flow through lines under this principle has led to ongoing discussions within the power system community on its theoretical rigorousness.

Another fundamental method proposed for PFT is the circuit theory approach, which focuses on the electrical characteristics of the network, such as current flows [7] and shunt admittances [8], and leverages principles like Thevenin's (or Norton's) equivalent circuit and basic circuit laws [9]. The strength of these methods lies in their ability to analyze power flows without relying on additional assumptions like the PSP. This could make it more robust. However, a major drawback is their inability to be universally applied across all test systems because of the requirement of complex transformations into equivalent circuits, assuming all system parameters are fully known.

Several researchers have applied graph theory principles to PFT [10]. These methods treat power systems as a graph and define modified incidence matrices to model the connection of buses (as nodes) with lines (as edges). [11] developed a graph-theory-based method to determine the contribution of generators and loads in line flows which provides the power transfer from generators to the loads. The proposed method's effectiveness is based on assumptions, such as PSP and the priority of generators to supply power loads on the same buses, which may not always reflect the actual power flow distribution in a network. This limitation has been partially addressed in [12] by defining an extended incidence matrix (EIM) that no longer relies on PSP. Nevertheless, these graph-theory-based methods require both generation outputs and line flow data to determine PFT, necessitating the assumption of a lossless network, which introduces additional inaccuracies.

In response to the aforementioned limitations, our main contribution is to propose a novel path-based optimization approach for PFT that enables proper estimation of the range of energy sources to any loads, regardless of the homogeneous nature of electricity and the intricate interconnections within power systems. This framework can be applied to estimate the potential range of specific energy sources, such as RESs,

for "green hydrogen" production validation, ensuring that the generated hydrogen meets eligibility criteria for government tax credits. To enhance the robustness of our PFT method, we relax the conventional assumptions such as PSP and priority of generators to supply loads at the same buses.

The remainder of this paper is organized as follows. Section II presents the methodology, followed by simulation results and analyses in Section III. Section IV concludes the paper with insights and potential future research directions.

II. Methodology

We integrate economic dispatch (ED) in power DSs and network modeling techniques in transportation systems to develop a path-base optimization model for PFT to quantify the minimum and maximum power flow from an energy source (e.g., RESs) to an energy load (e.g., hydrogen production). First, we present ED modeling within the distribution network in section II-A, aiming to minimize the generation cost from distributed generators (DGs) to serve the loads. Second, leveraging the path-link incidence matrix from graph theories, we construct feasible path flow sets so that we can identify the maximum and minimum power flow from generation nodes to end consumers in section II-B. The proposed methodology provides a valid way to justify the renewable energy share for power consumption to fulfill government tax credit requirements considering the topology and physical properties of DSs.

A. Economic Dispatch Modeling

The ED problem is central to power systems analyses, aiming to determine the most cost-effective generation scheduling from both DGs and substations that meet the power demand without violating DS operational constraints. The ED problem can be mathematically formulated in (1).

$$\min_{\substack{\boldsymbol{v},\boldsymbol{p},\boldsymbol{q}\geq\boldsymbol{0},\\ \boldsymbol{pf},\boldsymbol{qf}}} \quad \sum_{i\in\mathcal{I}^{\mathrm{DG}}}\sum_{t\in\mathcal{T}} C^{DG}_{i,t}p^{\mathrm{DG}}_{i,t} + \sum_{i\in\mathcal{I}^{\mathrm{Sub}}}\sum_{t\in\mathcal{T}} C^{Sub}_{i,t}p^{\mathrm{Sub}}_{i,t} \tag{1a}$$

$$\text{s.t.} \quad \sum_{l\in\mathcal{L}} pf_{l,t}\cdot \mathrm{LT}_{l,i} - \sum_{l\in\mathcal{L}} pf_{l,t}\cdot \mathrm{LF}_{l,i} = P^{d}_{i,t} - p^{\mathrm{DG}}_{i,t} - p^{\mathrm{Sub}}_{i,t}, \quad \forall i\in\mathcal{I}, t\in\mathcal{T} \tag{1b}$$

$$\sum_{l\in\mathcal{L}} qf_{l,t}\cdot \mathrm{LT}_{l,i} - \sum_{l\in\mathcal{L}} qf_{l,t}\cdot \mathrm{LF}_{l,i} = Q^{d}_{i,t} - q^{\mathrm{DG}}_{i,t} - q^{\mathrm{Sub}}_{i,t}, \quad \forall i\in\mathcal{I}, t\in\mathcal{T} \tag{1c}$$

$$pf^2_{l,t} + qf^2_{l,t} \leq (S^{\max}_{l})^2, \forall l\in\mathcal{L}, t\in\mathcal{T} \tag{1d}$$

$$v_{\mathrm{FN}_l,t} - v_{\mathrm{TN}_l,t} = 2\cdot(r_l\cdot pf_{l,t} + x_l\cdot qf_{l,t}), \quad \forall l\in\mathcal{L}, t\in\mathcal{T} \tag{1e}$$

$$(V^{\min})^2 \leq v_{i,t} \leq (V^{\max})^2, \ \forall i\in\mathcal{I}, t\in\mathcal{T}. \tag{1f}$$

DS is modeled as a directed graph $\mathcal{G}^P = (\mathcal{I}, \mathcal{L})$, where $\mathcal{I}$ (indexed with i) denotes the node set, which includes distributed generator (DG) nodes $\mathcal{I}^{\mathrm{DG}}$ and sub-station nodes $\mathcal{I}^{\mathcal{S}\sqcap\lfloor}$ as subsets; and L (indexed with l) denotes the line set. The objective (1a) aims to minimize the total generation cost from DGs and the energy purchase cost from sub-stations with $\boldsymbol{C}$ as the unit cost of energy. The constraints (1b) and (1c) ensure active/reactive power flow balance at each node by equating the net active/reactive power flow of lines ($\boldsymbol{pf}$) into node i with the net load at node i. LF (or TF) is the incidence matrices between lines and nodes, where its elements have a value of 1 if line l starts from (or connect to) node i and zero otherwise. The constraint (1d) prevents the apparent power flow on each distribution line from exceeding its maximum capacity ($\boldsymbol{S}^{\max}$), ensuring line safety and system stability. Constraint (1e) models the voltage difference between the endpoints of each line based on its electrical characteristics (reactance r and admittance x) and power flow, with $\boldsymbol{v}$ being squared of voltage magnitude and $\mathrm{FN}_l/\mathrm{TN}_l$ being the start/end nodes of each line l. Constraint (1f) ensures that the voltage at each node is within the specified bounds ($V^{\min}$, $V^{\max}$) to maintain power quality. These constraints are grounded in the Dist-Flow equations, which are widely adopted in distribution system modeling [13], [14].

B. Power Flow Tracing

1) Augment the DS as Bi-directional Graphs: We draw an analogy between generation-load in the DS network and origin-destination (OD) in the transportation network (TN) to facilitate the tracing of power flow. This approach allows us to model the flow of electricity in a manner similar to the movement of OD travel demand, providing an effective framework for analyzing the bounds of power flows from a generator to a demand node.

To form the topology of the DS as a bi-directional graph, we start by augmenting each distribution line with two directional links, as shown in Figure 1. Denote the resulting bi-directional graph as $\mathcal{G}^T = (\mathcal{I}, \mathcal{E})$, where $\mathcal{I}$ is the original node set in the DS, and $\mathcal{E}$ is the set of bi-directional edges. We follow the convention for the sign of power flow, i.e., power flow on line ij is positive when the power flows from the upstream node i to the downstream node j, and negative in the opposite direction. To explicitly represent the sign of power flows in $\mathcal{G}^T$, we impose the following conditions for each line l with upstream node i and downstream node j: (1) if the power flow is nonnegative ($pf_l \geq 0$), the link flow value connecting nodes i to j is set to pf_l and zero otherwise. Conversely, for negative power flow ($pf_l < 0$), the link flow value connecting nodes j to i is set to $-pf_l$ and zero otherwise.

In the next step, we assign generation and load nodes in DS as the origin and destination nodes in $\mathcal{G}^T$, respectively. Based on the defined ODs and links, we can generate all the possible paths between the origin and destination nodes. Since the DS is a tree network, there is only one path between each OD pair. However, our approach can be directly applied to transmission networks, where multiple paths are possible.

After generating the paths, we can form an incidence matrix A to describe the relation between the links and the paths. A is a $|\mathcal{E}| \times |\mathcal{P}|$ matrix where $|\mathcal{E}|$ is the number of edges and $|\mathcal{P}|$ is the number of paths. $a_{e,p}$ being an element of A will equal to 1 if link e is in the path p that connects origin r to destination s and will be zero otherwise.

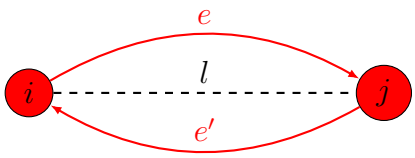

Fig. 1. Equivalent distribution line modeling with transportation directional links

2) Path flow optimization: After we construct $\mathcal{G}^T$ and associated link flow, denoted as $\boldsymbol{v}_{e,t}$, we can define optimization problems to maximize and minimize the potential path flow from a certain subset of origin nodes to a certain subset of destination nodes. For example, we can estimate the potential range of hydrogen production from RESs by the maximum and minimum possible path flow from origins with renewable energies (denoted as $\mathcal{I}^{\mathrm{RE}}$) to destinations with hydrogen production demand (denoted as $\mathcal{I}^{\mathrm{H}}$). This can be formulated as the optimization problem(s) (2).

$$\max / \min_{\boldsymbol{x} \geq \mathbf{0},} \quad \sum_{r \in \mathcal{I}^{\mathrm{RE}}, s \in \mathcal{I}^{H}} \sum_{p \in \mathcal{P}} \sum_{t \in \mathcal{T}} \delta_{r,s,p} x_{p,t} \tag{2a}$$

$$\text{s.t.} \quad \sum_{p \in \mathcal{P}} \mathrm{a}_{e,p} \cdot \mathrm{x}_{p,t} = v_{e,t}, \quad \forall e \in \mathcal{E}, t \in \mathcal{T} \tag{2b}$$

$$\sum_{t} x_{p,t} = C_p, \quad \forall p \in \mathcal{P}^C \tag{2c}$$

where, $\boldsymbol{x}$ represent the path flow; $\delta_{r,s,p}$ is a binary variable to indicate path p connect origin r and destination s; $\mathcal{P}^C$ is the set of paths connecting power sources and power loads with existing contracts; C_p is the contracted power supply of path p. The objective function (2a) aims to maximize/minimize the power transferred from renewable sources ($\mathcal{I}^{\mathrm{RE}}$) toward the nodes with hydrogen production ($\mathcal{I}^{H}$). Similar to traffic flow conservation in the transportation system, constraint (2b) models aggregation of flow on all paths using a particular link e should be equal to the link flow v_e; constraint (2c) guarantees that the power supply to a load equals the contracted amount.

III. Simulation Results and Analysis

In this section, we present the results of applying our path-based optimization approach for PFT to the IEEE-33 node test system. We focus on tracing the feasible power flow paths from RESs to nodes associated with hydrogen production and estimating the potential range of green hydrogen production. The algorithm was implemented using Pyomo 5.6.7 [15] and solved with IPOPT 3.12.

A. IEEE 33-node Test System

Our model was tested on the IEEE 33-node test system, as shown in Fig 2. In this distribution network, nodes 8, 13, and 30 serve as distributed generation nodes, with the system connected to the main grid at node 1 [16]. We considered node 8 to be connected to renewable DG.

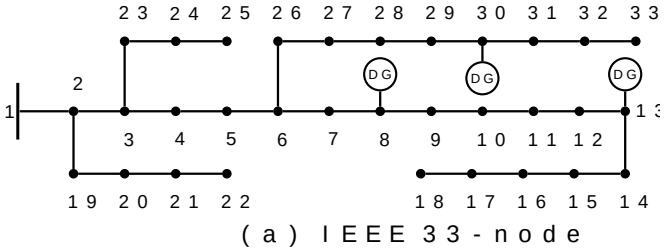

Fig. 2. IEEE-33 node test system

B. Renewable Energy Tracing

In this section, we concentrate on analyzing the power path flow from the renewable DG at node 8 to all load nodes, with a focus on identifying suitable locations for green hydrogen production. We aim to determine the potential renewable energy contribution to each node, which is essential for justifying the percentage of green hydrogen production. Table I summarizes the results on the maximum and minimum total renewable power flow to each node.

We observed that if hydrogen electrolyzers were installed at nodes 2, 4, 7, 8, and 25 (highlighted in green in Table I), these nodes received a maximum of 100% energy from renewable sources. However, different nodes had dramatically different lower bounds of renewable share. Fig 3 compares these 5 potential candidate locations for green hydrogen production. By considering both the maximum and minimum of renewable shares, we can determine the suitable sites for hydrogen production. For example, Node 2, with a maximum renewable supply of 100% and a minimum of 3%, was considered less favorable in the sense that this location is not easily justifiable for claiming tax credits due to the wider range of potential renewable shares. In contrast, Node 25 was identified as a more promising location due to its more consistent renewable energy shares, ranging from 73% to 100%. Node 8, while directly connected to renewable DG, only had 45% renewable shares in the minimum scenario because we relaxed the assumption that renewable energy would be prioritized for local power load. It is essential to note that green hydrogen production is not feasible at nodes 9 to 18 (highlighted in red in Table I), as there was no renewable energy contribution from DG 8 to these locations even considering the maximum scenario.

Figs 4a and 4b illustrate the maximum and minimum renewable shares at node 25 over 24-hour time steps. We observed that throughout the day, hydrogen production at node 25 is fully met by renewable energy from node 8 in the maximum scenario. In the minimum scenario, the majority of the energy demand came from renewable DG 8, while the remaining energy demand was served by node 13. These results suggest that installing hydrogen electrolyzers at node 25 is not sensitive to the time of day for green hydrogen production. If hydrogen production companies are going to convert conventional DGs to renewable ones, node 13 is a good candidate to increase the renewable shares of their hydrogen production.

TABLE I
THE RANGE OF RENEWABLE ENERGY CONTRIBUTION TO LOADS

Node ID	Max (pu)	Min (pu)	Total Load (pu)	Max/Total (%)	Min/Total (%)
2	1.960	0.065	1.960	100%	3%
3	1.764	0.024	1.764	100%	1%
4	2.352	0.185	2.352	100%	8%
5	1.176	0.000	1.176	100%	0%
6	1.176	0.000	1.176	100%	0%
7	3.920	1.764	3.920	100%	45%
8	3.920	1.764	3.920	100%	45%
9	0.000	0.000	1.176	0%	0%
10	0.000	0.000	1.176	0%	0%
11	0.000	0.000	0.882	0%	0%
12	0.000	0.000	1.176	0%	0%
13	0.000	0.000	1.176	0%	0%
14	0.000	0.000	2.352	0%	0%
15	0.000	0.000	1.176	0%	0%
16	0.000	0.000	1.176	0%	0%
17	0.000	0.000	1.181	0%	0%
18	0.000	0.000	1.764	0%	0%
19	1.764	0.024	1.764	100%	1%
20	1.764	0.024	1.764	100%	1%
21	1.764	0.024	1.764	100%	1%
22	1.764	0.024	1.764	100%	1%
23	1.764	0.024	1.764	100%	1%
24	0.329	0.000	0.329	100%	0%
25	8.232	6.035	8.232	100%	73%
26	1.057	0.000	1.176	90%	0%
27	1.021	0.000	1.176	87%	0%
28	0.941	0.000	1.176	80%	0%
29	1.548	0.130	2.352	66%	6%
30	1.306	0.231	3.920	33%	6%
31	1.049	0.000	2.940	36%	0%
32	1.353	0.263	4.116	33%	6%
33	0.491	0.000	1.176	42%	0%

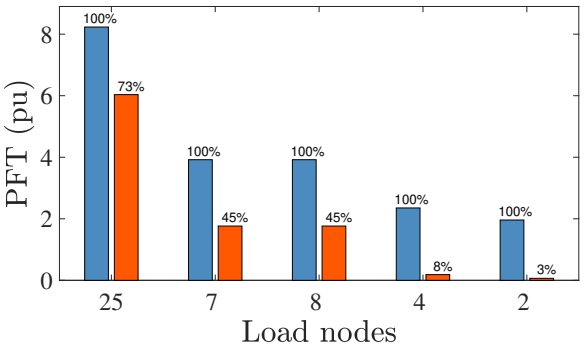

Fig. 3. PFT ranges from RES to candidate locations for green hydrogen production; max scenario and min scenario

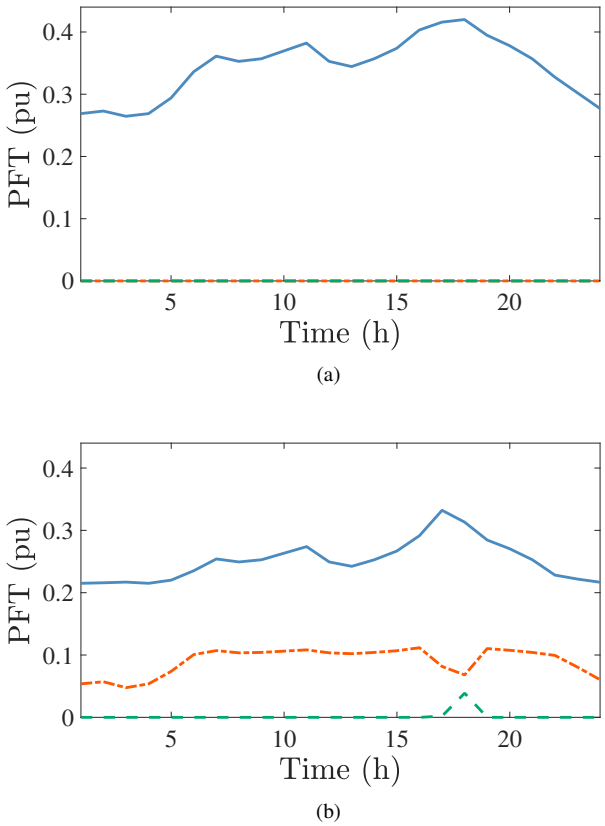

Fig. 4. Hourly PFT to load node 25; a) max scenario and b) min scenario from DG nodes: — 8, - - - 13, - - - 30.

To demonstrate the feasibility of the minimum and maximum scenarios outlined, we present a power flow tracing example from the renewable energy source (DG8) to candidate hydrogen node (node 25) at time step $t = 18$. This specific time step was chosen due to its peak load. The green arrow indicates the power flow direction for each line. The numbers in blue and red represent the power supplied by DG8 to these nodes under the minimum and maximum scenarios from node 8 to node 25, respectively. In both scenarios, the total energy output from DG8 remains constant (1.61 pu). In the maximum scenario, node 8's load is partially supplied by the power from node 9 to node 8 (which is 0.07 pu generated from DG 13), in which case the power flow from node 24 to node 25 is entirely from node 8. Therefore, node 25 receive 0.42 pu from DG 8. In the minimum scenario, the power flow from node 24 to node 25 has 0.11 pu from non-renewable DGs, which include 0.04 pu from DG 30 (since 0.04 pu from node 26 to 6) and 0.07 pu from DG 13 (since 0.07 pu from node 9 to node 8). This result underscores the effectiveness of the proposed Power Flow Tracing (PFT) method in assessing the potential range of energy delivery from the renewable energy source.

IV. CONCLUSION

This study develops a path-based optimization approach for PFT in power DSs to effectively estimate the upper and lower bounds of OD flow. We demonstrate the methodology

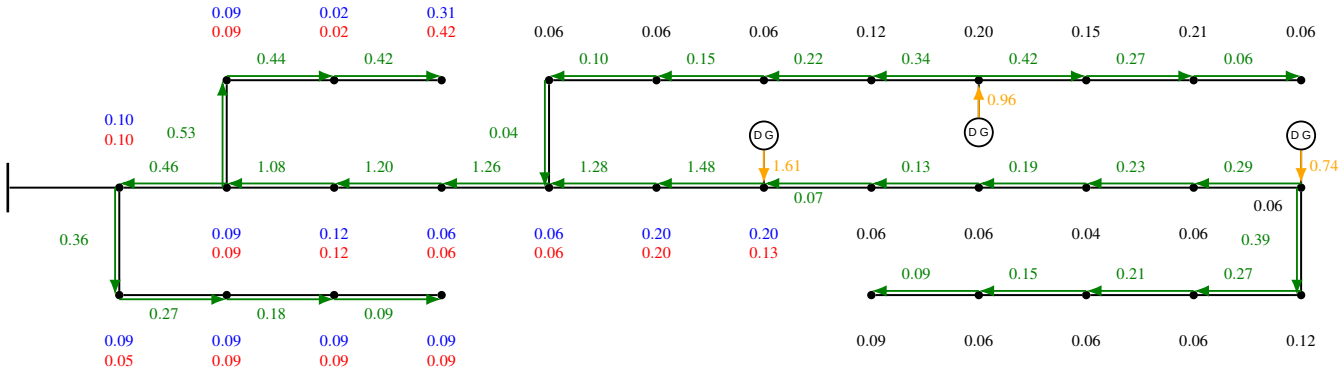

Fig. 5. Power flow at time $t = 18$, with node 25 as the candidate hydrogen node, where $\rightarrow$ shows the line power flow,$\rightarrow$ shows the generation output of DGs. The (blue) and (red) numbers indicate the load contributions from RE (DG 8) for the minimum and maximum scenarios, respectively; Numbers in (black) show the load demand w/o renewable energy contribution.

in the context of quantifying the shares of RESs for hydrogen production. By applying the methodology to the IEEE-33 node test system, we identify Node 25 as a promising location for green hydrogen production due to its high and consistent renewable energy shares. Our findings emphasize the importance of robust PFT in identifying suitable locations for green hydrogen production to support the transition towards a net-zero carbon infrastructure. Future work can focus on extending the methodology to more complex network topologies, optimizing the green hydrogen production sites, and conducting economic analyses to incentivize the usage of RESs in hydrogen production.

REFERENCES

[1] U.S. Department of Energy, "Hydrogen production: Electrolysis," https://www.energy.gov/eere/fuelcells/hydrogen-production-electrolysis, 2021, accessed: 2023-02-09.

[2] Davis Wright Tremaine LLP, "Clean energy tax credits available to tax-exempt and governmental entities under the inflation reduction act," https://www.dwt.com/insights/2023/09/clean-energy-tax-credits-nonprofits-tax-exempt-ira, 2023, accessed: 2023-02-09.

[3] J. Bialek, "Tracing the flow of electricity," *IEE Proceedings - Generation, Transmission and Distribution*, vol. 143, no. 4, pp. 313–320, 1996.

[4] E. Vega-Fuentes, J. Yang, C. Lou, and N. K. Meena, "Transaction-oriented dynamic power flow tracing for distribution networks—definition and implementation in gis environment," *IEEE Transactions on Smart Grid*, vol. 12, no. 2, pp. 1303–1313, 2021.

[5] A. Dargahi, K. Sanjani, M. Nazari-Heris, B. Mohammadi-Ivatloo, S. Tohidi, and M. Marzband, "Scheduling of air conditioning and thermal energy storage systems considering demand response programs," *Sustainability*, vol. 12, no. 18, p. 7311, 2020.

[6] K. Sanjani, B. Mohammadi-Ivatloo, M. Marzband, M. Shafiee, and A. Anvari-Moghaddam, "Robust self-scheduling of a large solar producer coupled with battery storage system," in *10th International Conference on Power Electronics, Machines and Drives, PEMD 2020*. IEEE Press, 2020, pp. 1–6.

[7] A. Leite da Silva and J. G. de Carvalho Costa, "Transmission loss allocation: part i-single energy market," *IEEE Transactions on Power Systems*, vol. 18, no. 4, pp. 1389–1394, 2003.

[8] A. J. Conejo, J. Contreras, D. A. Lima, and A. Padilha-Feltrin, "Z_{bus} transmission network cost allocation," *IEEE Transactions on Power Systems*, vol. 22, no. 1, pp. 342–349, 2007.

[9] C. Wang, Y. Wang, M. Rouholamini, and C. Miller, "An equivalent circuit-based approach for power and emission tracing in power networks," *IEEE Systems Journal*, vol. 16, no. 2, pp. 2206–2216, 2021.

[10] K. Berg, "Power flow tracing: Methods and algorithms," Master's thesis, Norwegian University of Science and Technology, 2017.

[11] F. F. Wu, Y. Ni, and P. Wei, "Power transfer allocation for open access using graph theory-fundamentals and applications in systems without loopflow," *IEEE transactions on power systems*, vol. 15, no. 3, pp. 923–929, 2000.

[12] K. Xie, J. Zhou, and W. Li, "Analytical model and algorithm for tracing active power flow based on extended incidence matrix," *Electric Power Systems Research*, vol. 79, no. 2, pp. 399–405, 2009.

[13] M. E. Baran and F. F. Wu, "Network reconfiguration in distribution systems for loss reduction and load balancing," *IEEE Power Engineering Review*, vol. 9, no. 4, pp. 101–102, 1989.

[14] D. K. Molzahn, F. Dörfler, H. Sandberg, S. H. Low, S. Chakrabarti, R. Baldick, and J. Lavaei, "A survey of distributed optimization and control algorithms for electric power systems," *IEEE Transactions on Smart Grid*, vol. 8, no. 6, pp. 2941–2962, 2017.

[15] M. L. Bynum, G. A. Hackebeil, W. E. Hart *et al.*, *Pyomo–optimization modeling in python*, 3rd ed. Springer Science & Business Media, 2021, vol. 67.

[16] S. Baghali, Z. Guo, W. Wei, and M. Shahidehpour, "Electric vehicles for distribution system load pickup under stressed conditions: A network equilibrium approach," *IEEE Transactions on Power Systems*, vol. 38, no. 3, pp. 2304–2317, 2022.